

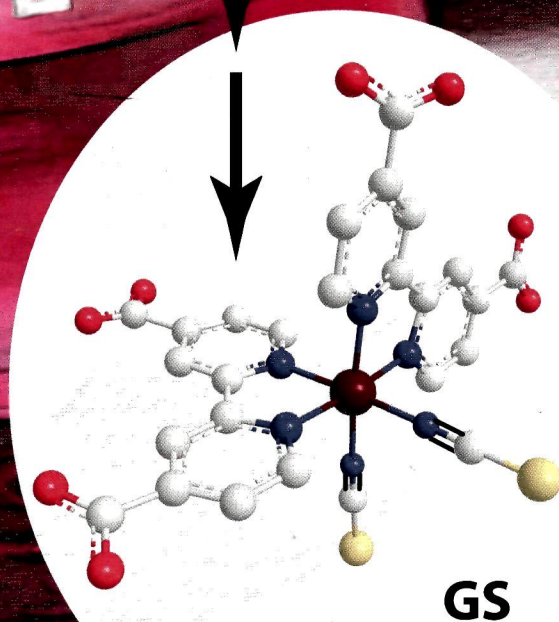
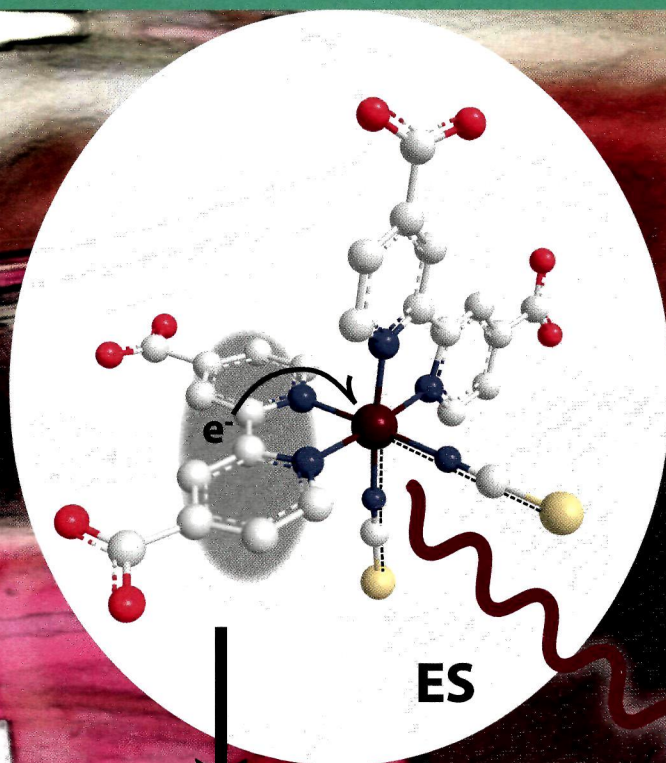
111
1-65

Inorganic Chemistry

including bioinorganic chemistry

June 17, 2013
Volume 52, Number 12
pubs.acs.org/IC

Excited-State Relaxation of Ruthenium Polypyridyl Compounds



ACS Publications
MOST TRUSTED. MOST CITED. MOST READ.

www.acs.org

ON THE COVER: Variable-temperature photoluminescence studies were performed on ruthenium polypyridyl compounds relevant to dye-sensitized solar cells in order to identify their excited-state relaxation pathways in fluid solution and anchored to mesoporous TiO_2 or ZrO_2 thin films. See R. M. O'Donnell, P. G. Johansson, M. Abrahamsson, and G. J. Meyer, p 6839.

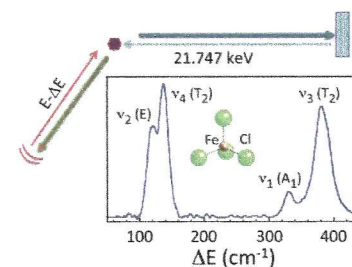
Communications

 6767 **S**
dx.doi.org/10.1021/ic400353j

Inelastic X-ray Scattering of a Transition-Metal Complex (FeCl_4^-): Vibrational Spectroscopy for All Normal Modes

Weibing Dong, Hongxin Wang, Marilyn M. Olmstead, James C. Fetting, Jay Nix, Hiroshi Uchiyama, Satoshi Tsutsui, Alfred Q. R. Baron, Eric Dowty, and Stephen P. Cramer*

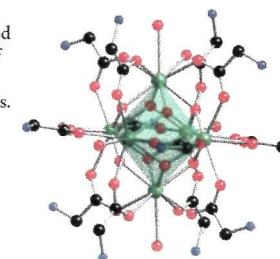
Inelastic X-ray scattering (IXS) has been used to characterize the normal modes of $(\text{NET}_4)(\text{FeCl}_4)$, a feasibility test for other complex transition-metal complexes. Using an incoming photon energy of 21.747 keV, an overall resolution of 1.5 meV (12 cm^{-1}) was achieved. IXS has the advantage that all normal modes can be observed for a sample with any elemental composition. There should be applications in coordination chemistry where this technique complements other vibrational spectroscopies.


 6770 **S**
dx.doi.org/10.1021/ic4007185

Plutonium(IV) Cluster with a Hexanuclear $[\text{Pu}_6(\text{OH})_4\text{O}_4]^{12+}$ Core

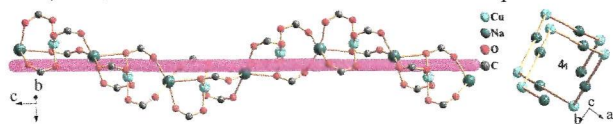
Karah E. Knope* and L. Soderholm

Evaporation of an acidic aqueous plutonium(IV) solution containing glycine ligands yielded $\text{Li}_6[\text{Pu}_6(\text{OH})_4\text{O}_4(\text{H}_2\text{O})_6(\text{HGly})_{12}]\text{Cl}_{18} \cdot 10.5\text{H}_2\text{O}$ (**1**), which consists of a mixed hydroxo/oxoplutonium(IV) hexanuclear cluster. The hexanuclear unit is a product of plutonium(IV) hydrolysis and condensation and represents the first example of a plutonium(IV) polynuclear complex containing both hydroxo- and oxo-bridging ligands.

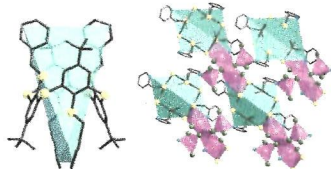


Chiral Induction in the Ionothermal Synthesis of a 3D Chiral Heterometallic Metal–Organic Framework Constructed from Achiral 1,4-Naphthalenedicarboxylate

Qing-Yan Liu,* Wei-Lu Xiong, Cai-Ming Liu, Yu-Ling Wang, Jia-Jia Wei, Zuo-Juan Xiahou, and Li-Hua Xiong

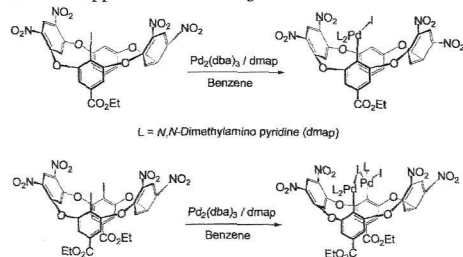
Induction of a chiral compound, [(EMIM)NaCu(1,4-ndc)₂]_n (**1**; 1,4-ndc = 1,4-naphthalenedicarboxylate), by an enantiopure 1-ethyl-3-methylimidazolium (EMIM) l-lactate additive under ionothermal conditions is presented.**Molecular Tectonics: Control of the Dimensionality in Tetramercaptothiacalixarenes Based Coordination Networks**

A. Ovsyannikov, S. Ferlay,* S. E. Solovieva, I. S. Antipin, A. I. Kononov, N. Kyritsakas, and M. W. Hosseini*

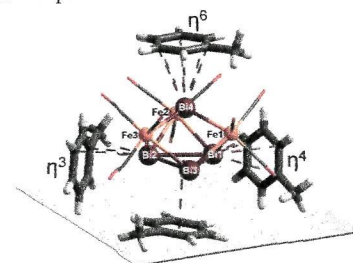
Combinations of tetramercaptothiacalix[4]arene pyridyl-appended positional isomers with HgCl₂ lead to the formation of three new neutral coordination networks with imposed 1–3D dimensionality by the position of the N atom on the pyridyl group.**Organopalladium Complexes of Oxacalixarenes: Selecting the Lid for the Three-Dimensional Scaffold**

Yulia Visitaev, Israel Goldberg, and Arkadi Vigalok*

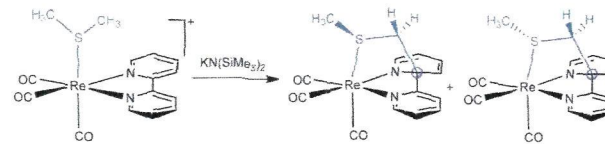
Palladium(II) atoms can be directly attached to either one or two aromatic rings of the three-dimensional oxacalixarene scaffold. When the appropriate ligands were chosen, it was possible to place them at the top of the calixarene cavity or make them interact with the substituent at the opposite aromatic ring.

**Synthesis and Crystal Structure of a “FeBi” Cluster Compound with Noncovalent Low-Valent Bi···π_{Arene} Interactions**

Kirill Yu. Monakhov,* Christophe Gourlaouen, Thomas Zessin, and Gerald Linti

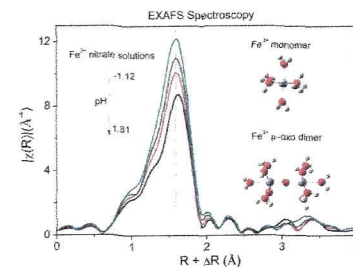
The electronic structure features of the synthesized [Bi₄Fe₂(CO)₉] cluster give rise to “extra” supramolecular chemistry for the low-valent Bi atoms, offering unique types of noncovalent Bi···π_{arene} and ΔBi···π_{arene} interactions where the coordination modes of the PhMe rings involve various hapticities.

Rebeca Arévalo, Julio Pérez,* and Lucía Riera

Treatment with KN(SiMe₃)₂ in tetrahydrofuran deprotonates one of the CH₃ groups of the coordinated dimethyl sulfide in [Re(bipy)(CO)₃(SMe₂)](OTf) (**1**). In the product, a mixture of diastereomers (**2M** and **2m**), the so-generated methylene group is coupled to the C2 atom of one of the 2-pyridyl groups of 2,2'-bipyridine and, as a result, is dearomatized. Employing a 2,6-^tPr-BIAN (instead of 2,2'-bipyridine) derivative yielded a similar product, which could be fully characterized including X-ray diffraction.**Articles****In Situ Structural Characterization of Ferric Iron Dimers in Aqueous Solutions: Identification of μ-Oxo Species**

Mengqiang Zhu, Brendan W. Puls, Cathrine Frandsen, James D. Kubicki, Hengzhong Zhang, and Glenn A. Waychunas*

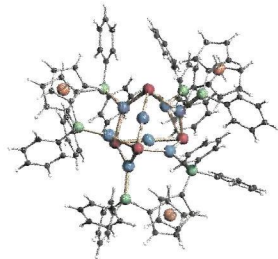
The structure of the ferric iron dimer in aqueous nitrate solutions has been characterized in situ using Fe K-edge EXAFS spectroscopy. Results convincingly show that the dimer takes the μ-oxo form rather than the dihydroxo form, solving the long-standing controversy over the dimer structure.



6798 **S** dx.doi.org/10.1021/ic3021854

Copper Chalcogenide Clusters Stabilized with Ferrocene-Based Diphosphine Ligands
Chhatra B. Khadka, Bahareh Khalili Najafabadi, Mahdi Hesari, Mark S. Workentin,* and John F. Corrigan*

1,1'-Bis(diphenylphosphino)ferrocene (dppf) has been used to stabilize a series of copper(I) chalcogenide clusters. Single-crystal X-ray analyses of the complexes confirm the presence of $\{Cu_2E_2\}$ cores (E = S, Se, Te) with dppf ligands on their surfaces, where the bidentate ligands adopt bridging coordination modes.

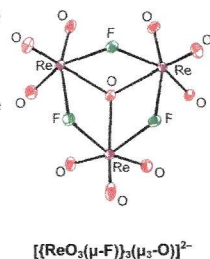


6806 **S** dx.doi.org/10.1021/ic302221y

Synthesis and Lewis Acid Properties of $(ReO_3F)_\infty$ and the X-ray Crystal Structures of $(HF)_2ReO_3F \cdot HF$ and $[N(CH_3)_4]_2[ReO_3(\mu-F)(\mu_3-O)] \cdot CH_3CN$

Maria V. Ivanova, Tobias Köchner, H  lene P. A. Mercier, and Gary J. Schrobilgen*

Solvolytic of Re_2O_7 in anhydrous HF (aHF) in the presence of F_2 gas provides a reliable synthesis of high-purity $(ReO_3F)_\infty$. Dissolution of $(ReO_3F)_\infty$ in aHF yielded $(HF)_2ReO_3F \cdot HF$, in which two of the HF molecules are coordinated to rhenium through their fluorine atoms. Reaction of $[N(CH_3)_4][F]$ with $(ReO_3F)_\infty$ in CH_3CN yielded $[ReO_3(\mu-F)(\mu_3-O)]^{2-}$, which contains a central oxygen-bridge atom equivalently bonded to three rhenium atoms. The rhenium atoms are bridged to one another by three fluorine-bridge atoms.

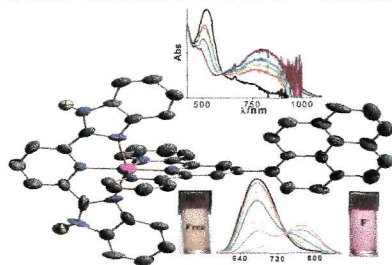


6820 **S** dx.doi.org/10.1021/ic3022326

Synthesis, Structural Characterization, and Photophysical, Spectroelectrochemical, and Anion-Sensing Studies of Heteroleptic Ruthenium(II) Complexes Derived from 4'-Polyaromatic-Substituted Terpyridine Derivatives and 2,6-Bis(benzimidazol-2-yl)pyridine

Dinesh Maity, Shyamal Das, Sourav Mardanya, and Sujoy Baitalik*

Luminescent heteroleptic bis-tridentate Ru(II) complexes derived from 4'-polyaromatic-substituted terpyridines and bis(benzimidazolyl)pyridine can act as multichannel sensors for selective anions in solution through different channels.

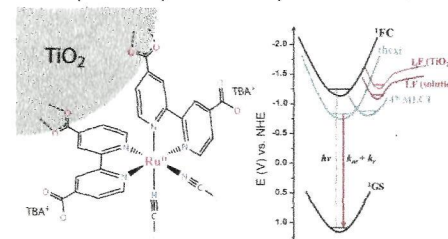


6839 dx.doi.org/10.1021/ic302339a

Excited-State Relaxation of Ruthenium Polypyridyl Compounds Relevant to Dye-Sensitized Solar Cells

Ryan M. O'Donnell, Patrik G. Johansson, Maria Abrahamsson, and Gerald J. Meyer*

Variable-temperature photoluminescence studies of compounds of the general type $cis-Ru(LL)_2(NCS)_2$ anchored to mesoporous TiO_2 thin films displayed behavior consistent with excited-state relaxation through an upper excited state, indicating that ligand loss photochemistry is unlikely to occur in dye-sensitized solar cells.

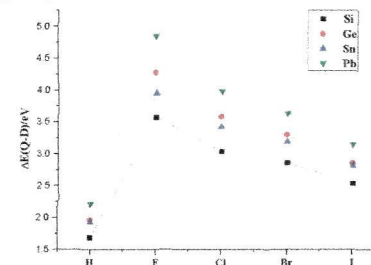


6849 dx.doi.org/10.1021/ic3025099

Diatomic Silylynes, Germylynes, Stannylynes, and Plumbylynes: Structures, Dipole Moments, Dissociation Energies, and Quartet-Doublet Gaps of EH and EX (E = Si, Ge, Sn, Pb; X = F, Cl, Br, I)

Huidong Li, Hao Feng,* Weiguo Sun, Yaoming Xie, and Henry F. Schaefer*

The $^3\Pi$ state is the ground electronic state for the carbyne and halocarbene analogues E-H and E-X (E = Si, Ge, Sn, Pb; X = F, Cl, Br, I). The quartet-doublet splittings fall in the order $EF > ECl > EBr > EI > EH$ for a given metal E; and $PbX > GeX > SnX > SiX$ for the same halogen atom X.

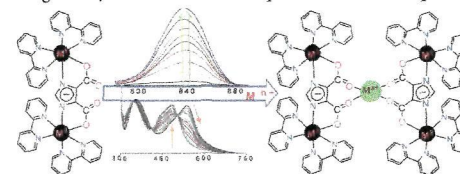


6860 **S** dx.doi.org/10.1021/ic302566p

A Combined Experimental and DFT/TD-DFT Investigation of Structural, Electronic, and Cation-Induced Switching of Photophysical Properties of Bimetallic Ru(II) and Os(II) Complexes Derived from Imidazole-4,5-Dicarboxylic Acid and 2,2'-Bipyridine

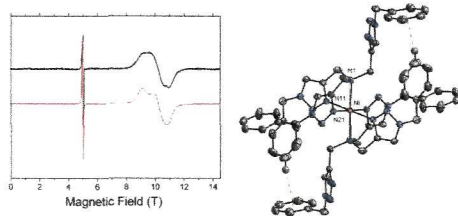
Shyamal Das, Srikanta Karmakar, Debasish Saha, and Sujoy Baitalik*

The structural, electronic, and cation-induced luminescence switching behaviors of mixed-ligand bimetallic ruthenium(II) and osmium(II) complexes were investigated by a combination of experimental and computational methods.

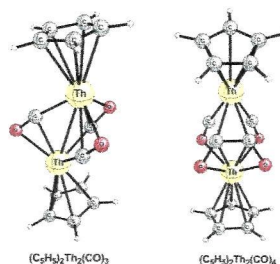


Electronic Structures of Octahedral Ni(II) Complexes with "Click" Derived Triazole Ligands: A Combined Structural, Magnetometric, Spectroscopic, and Theoretical Study

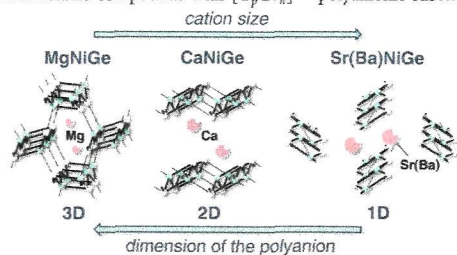
David Schweinfurth, J. Krzystek,* Igor Schapiro, Serhiy Demeshko, Johannes Klein, Joshua Telser,* Andrew Ozarowski, Cheng-Yong Su, Franc Meyer, Mihail Atanasov,* Frank Neese,* and Biprajit Sarkar*

A series of mononuclear octahedral Ni(II) complexes with tripodal and bidentate "Click" derived substituted 1,2,3-triazole ligands are presented. A battery of techniques such as x-ray crystallography, SQUID magnetometry, HFEP spectroscopy, and LFT and *ab initio* calculations have been used to elucidate the electronic structures of these complexes.**Extreme Metal Carbonyl Back Bonding in Cyclopentadienylthorium Carbonyls Generates Bridging C₂O₂ Ligands by Carbonyl Coupling**

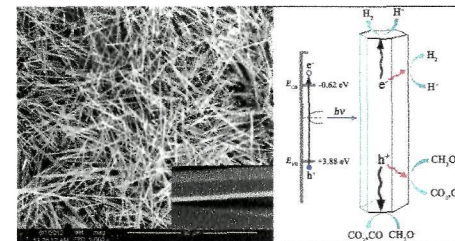
Huidong Li, Hao Feng,* Weiguo Sun, R. Bruce King,* and Henry F. Schaefer III

The most favorable Cp₂Th₂(CO)_n (n = 2 to 5) structures in terms of energy and thermochemistry are the tricarbonyl Cp₂Th₂(η²-μ-CO)₃ and the tetracarbonyl Cp₂Th₂(η¹-μ-C₂O₂)(η²-μ-CO)₂. These species add CO to form Cp₂Th₂(CO)₅ structures with relatively weakly bound terminal CO groups. The bridging CO groups in these structures exhibit unusually low ν(CO) frequencies down to 1167 cm⁻¹ indicating extremely strong Th→CO back bonding.**From One to Three Dimensions: Corrugated ¹[NiGe] Ribbons as a Building Block in Alkaline Earth Metal Ae/Ni/Ge Phases with Crystal Structure and Chemical Bonding in AeNiGe (Ae = Mg, Sr, Ba)**

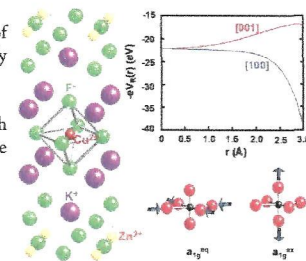
Viktor Hlukhyy, Lisa Siggelkow, and Thomas F. Fässler*

Increasing the cation size leads to a reduction of the dimension of [NiGe] polyanions in equiatomic alkaline earth nickel germanides AeNiGe (Ae = Mg, Ca, Sr, Ba). The ¹[NiGe] ribbons as they occur as isolated strands in Sr(Ba)NiGe are the basic building blocks in many intermetallic compounds with [T_nGe_n]^{m-} polyanionic substructures (T = transition metal).**A Template-Free Solution Route for the Synthesis of Well-Formed One-Dimensional Zn₂GeO₄ Nanocrystals and Its Photocatalytic Behavior**

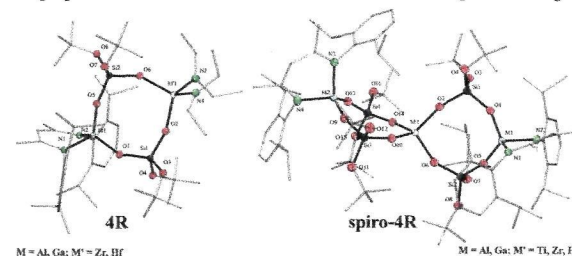
Jun Liang, Yiqun Cao, Huan Lin, Zizhong Zhang, Changcang Huang, and Xuxu Wang*

Well-formed Zn₂GeO₄ hexagonal nanorods and nanofibers with high aspect ratios were readily obtained by a template-free solution route. The prismatic Zn₂GeO₄ nanocrystals are uniform single crystal with the longitudinal direction along the [001] and were dominated by (110) and (110) surfaces. The obtained samples exhibit an excellent H₂-evolving activity by a water splitting reaction in the presence of methanol under UV-light irradiation. Furthermore, this successful synthetic strategy is expected to be utilized in the large-scale preparation of single-crystalline Zn₂GeO₄ hexagonal 1-D nanomaterials.**Cu²⁺ in Layered Compounds: Origin of the Compressed Geometry in the Model System K₂ZnF₄:Cu²⁺**

J. A. Aramburu,* J. M. García-Lastra, P. García-Fernández, M. T. Barriuso, and M. Moreno

The microscopic origin of the unusual tetragonal compressed geometry of CuF₆⁴⁻ complexes formed in Cu²⁺-doped K₂ZnF₄ layered perovskite is explored by means of *ab initio* calculations. It is shown that the compressed geometry of this center is mainly determined by the anisotropic electric field produced by the rest of the ions of the tetragonal K₂ZnF₄ lattice on the complex. Moreover, the small distortion of the complex (R_{ax} - R_{eq} = 11 pm) is not due to a JT effect but to a vibronic coupling with two symmetric a_{1g} modes, which does not give rise to any symmetry breaking of the CuF₆⁴⁻ complex subject to the internal field of the host lattice.**Heterometallic Alumo- and Gallodisilicates with M(O-Si-O)₂M' and [M(O-Si-O)₂]₂M' Cores (M = Al, Ga; M' = Ti, Zr, Hf)**

Raúl Huerta-Lavorie, Diego Solís-Ibarra, Dana Victoria Báez-Rodríguez, Marisol Reyes-Lezama, M. de las Nieves Zavala-Segovia, and Vojtech Jancik*

Molecular alumo- or gallodisilicates [HC{C(Me)N(2,6-iPr₂C₆H₃)₂}]₂M[(μ-O)Si(OtBu)₂(OH)]₂ (M = Al, Ga) have been synthesized and used in the preparation of heterobimetallic disilicates with 4R and spiro-4R inorganic cores of up to 0.81 nm.

6944

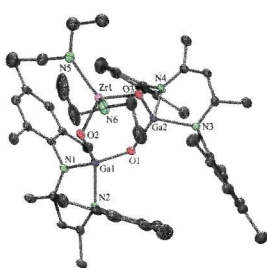


dx.doi.org/10.1021/ic4010054

A Synthetic Route to a Molecular Galloxane Dihydroxide and Its Group 4 Heterobimetallic Compounds

Erandi Bernabé-Pablo, Vojtech Jancik, and Mónica Moya-Cabrera*

The molecular galloxane dihydroxide $[\{^{\text{Me}}\text{LGa}(\text{OH})\}_2(\mu\text{-O})]$ (**2**) was prepared by the controlled hydrolysis of $[\text{Me}^{\text{L}}\text{GaCl}_2]$ (**1**) using a NHC carbene as a HCl acceptor. This synthetic approach allowed the preparation of molecular heterobimetallic galloxanes derived from group 4 metals and 2. An alternative approach was used to prepare the galloxane dichloride $[\{^{\text{Me}}\text{LGa}(\text{Cl})\}_2(\mu\text{-O})]$ (**3**), and its reduction with $\text{AlH}_3 \cdot \text{NMe}_3$ led to the monometallic gallium hydride $[\text{Me}^{\text{L}}\text{LGaH}_2]$ (**4**).



6951

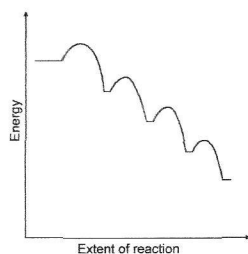


dx.doi.org/10.1021/ic4009366

Cluster Harvesting by Successive Reduction of a Metal Halide with a Nonconventional Reduction Agent: A Benefit for the Exploration of Metal-Rich Halide Systems

Markus Ströbele, Agnieszka Mos, and Hans-Jürgen Meyer*

The formation of metastable compounds was monitored for two series of tungsten halides. With a new scanning technique that we call *Cluster Harvesting*, a whole sequence of compounds is monitored when departing from a reactive starting material and a reduction agent, as we describe in detail for tungsten halide systems.



6957

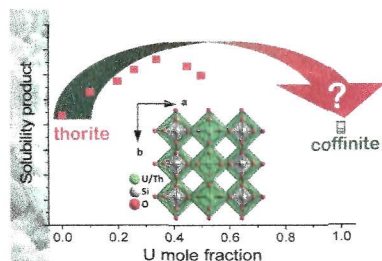


dx.doi.org/10.1021/ic400272s

From Uranothorites to Coffinite: A Solid Solution Route to the Thermodynamic Properties of USiO_4

Stéphanie Szenknect*, Dan T. Costin, Nicolas Clavier, Adel Mesbah, Christophe Poinssot, Pierre Vitorge, and Nicolas Dacheux

Experiments on the solubility of intermediate members of the $\text{Th}_{1-x}\text{U}_x\text{SiO}_4$ solid solution were carried out to determine the impact of Th–U substitutions on the thermodynamic properties of the solid solution and then allow extrapolation to the coffinite end member. Our data at low temperature clearly show that uranothorite solid solutions with $x > 0.26$, thus coffinite, are less stable than the mixture of binary oxides, which is consistent with qualitative evidence from petrographic studies of uranium ore deposits.



6969



dx.doi.org/10.1021/ic400302e

Synthesizing Axial Inserting p–n Heterojunction Nanowire Arrays for Realizing Synergistic Performance

Haowei Lin, Huibiao Liu,* Xuemin Qian, Songhua Chen, Yongjun Li, and Yuliang Li*

Consideration of the material design and components match on structure and energy, the solid–solid combined nanowires of p-type conductive polymer of PTCM and n-type inorganic semiconductor PbS was prepared with a $2.57 \mu\text{m}^2$ heterojunction interface. The axial deeply inserting heterojunction nanowire arrays exhibited excellent rectifying features and diode nature, as well as obvious electrical switching behavior, which are much excelled individual components of PTCM and PbS nanowire arrays for realizing synergistic performance.



6975

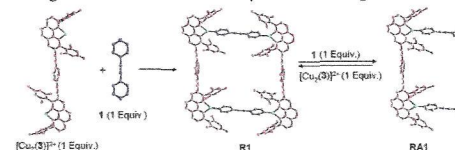


dx.doi.org/10.1021/ic400328d

Heteroleptic Metallosupramolecular Racks, Rectangles, and Trigonal Prisms: Stoichiometry-Controlled Reversible Interconversion

Subhadip Neogi,* Yvonne Lorenz, Marianne Engeser, Debabrata Samanta, and Michael Schmittel*

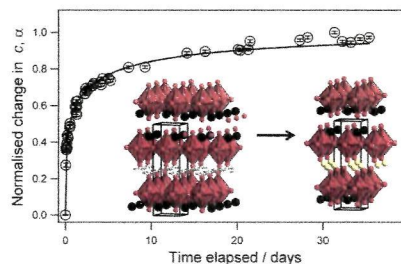
Utilization of the HETPYP-I (HETeroleptic PYridyl and Phenanthroline metal complexes) complexation strategy allows for the three-component self-assembly of a series of discrete supramolecular rectangles and trigonal prisms. As a proof of their dynamic nature, the reversible supramolecule-to-supramolecule interconversion of discrete rectangles and rack architectures was isdemonstrated, simply by tuning the relative stoichiometry of their components.



Ion Exchange and Structural Aging in the Layered Perovskite Phases $H_{1-x}Li_xLaTiO_4$

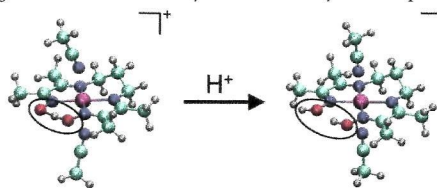
T. W. S. Yip and E. J. Cussen*

Grinding together the layered solid acid $HLaTiO_4$ with stoichiometric quantities of lithium hydroxide monohydrate gives the solid solution $H_{1-x}Li_xLaTiO_4$. The reaction proceeds rapidly, but the unit cell size continues to evolve over the course of days with a gradual compression along the interlayer direction that can be modeled using a power law dependence reminiscent of an Ostwald ripening process. On heating, these materials undergo a mass loss because of dehydration but retain the layered Ruddlesden–Popper structure up to 480°C .

**Effects of Ligand Modification and Protonation on Metal Oxime Hydrogen Evolution Electrocatalysts**

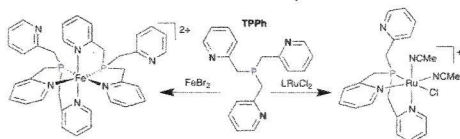
Brian H. Solis, Yinxi Yu, and Sharon Hammes-Schiffer*

The design of hydrogen-evolving electrocatalysts that operate at modest overpotentials is important for solar energy devices. Calculations of reduction potentials and pK_a 's for Co, Ni, and Fe diimine-dioxime and diglyoxime complexes elucidate the impact of modification and protonation of the oxime bridge. Asymmetric complexes containing a single O–H–O bridge are proposed to be effective hydrogen evolution electrocatalysts with relatively low overpotentials in acetonitrile and water.

**Tri(pyridylmethyl)phosphine: The Elusive Congener of TPA Shows Surprisingly Different Coordination Behavior**

Christopher J. Whiteoak, James D. Nobbs, Evgeny Kiryushchenkov, Sandro Pagano, Andrew J.P. White, and George J.P. Britovsek*

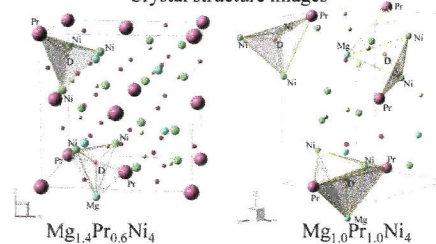
Tri(pyridylmethyl)phosphine (TPPh), the remarkably elusive congener of tri(pyridylmethyl)amine (TPA), has been prepared, as well as the relative tri(*N*-methyl-pyridylamino)phosphine (TPAMP). The coordination properties of these new ligands have been evaluated for chromium(III), iron(II), and ruthenium(II) complexes and compared with the related TPA complexes. In all cases, a different coordination behavior has been observed whereby TPPh and TPAMP always act as tridentate ligands.

**Crystal Structure and Local Structure of $Mg_{2-x}Pr_xNi_4$ ($x = 0.6$ and 1.0) Deuteride Using In Situ Neutron Total Scattering**

K. Sakaki,* N. Terashita, H. Kim, T. Proffen, E. H. Majzoub, S. Tsunokake, Y. Nakamura, and E. Akiba

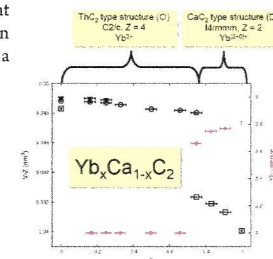
We studied crystal structure and local structure of $Mg_{2-x}Pr_xNi_4$ ($x = 0.6$ and 1.0) and their deuterides using in situ neutron total scattering and first-principles calculations. The total scattering data were analyzed using Rietveld refinement and pair distribution function analysis (PDF). The crystal structure of $Mg_{2-x}Pr_xNi_4$ before deuterium absorption was $C15b$ in space group $F\bar{4}3m$. No difference between the crystal and local (PDF) structures was observed. The crystal structure of $Mg_{1.0}Pr_{1.0}Ni_4D_{2-4}$ was found to be orthorhombic in space group $Pmn2_1$, with three deuterium occupation sites: $PrNi_3$ and two types of bipyramidal Pr_2MgNi_2 that have a plane of symmetry composed of $MgNi_2$.

Crystal structure images

**Structure Induced Yb Valence Changes in the Solid Solution $Yb_xCa_{1-x}C_2$**

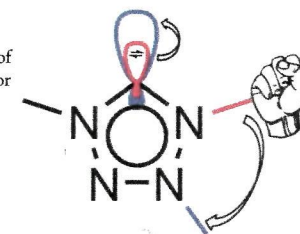
Pascal Link, Pieter Glatzel, Kristina Kvashnina, Dmytro M. Trots, Ronald I. Smith, and Uwe Ruschewitz*

The solid solution $Yb_xCa_{1-x}C_2$ ($0 \leq x \leq 1$) was synthesized by reaction of the elements at 1323 K. The crystal structures within this solid solution, as elucidated from synchrotron powder diffraction data, depend on x and exhibit some interesting features that point to a structure dependent valence state of Yb.

**Synthesis and Comparison of Transition Metal Complexes of Abnormal and Normal Tetrazolyidenes: A Neglected Ligand Species**

Lars-Arne Schaper, Xuhui Wei, Philipp J. Altmann, Karl Öfele, Alexander Pöthig, Markus Drees, János Mink, Eberhardt Herdtweck, Bettina Bechlers, Wolfgang A. Herrmann, and Fritz E. Kühn*

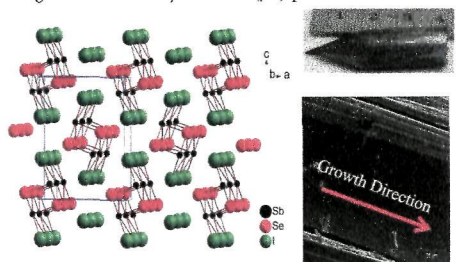
“Me” makes all the difference: By changing the substitution pattern of methyl substituents in tetrazolyidenes from 1,4- to 1,3-position, a significant leverage in σ -donor strength of the carbene ligands can be provoked. This is observed in a variety of novel transition metal complexes, synthesized via the corresponding silver carbene or using precursors equipped with internal base, by means of detailed spectroscopic examinations, as well as DFT calculations.



7045 dx.doi.org/10.1021/ic401086r

Photoconductivity in the Chalcogenide Semiconductor, SbSeI: a New Candidate for Hard Radiation Detection
 Arief C. Wibowo, Christos D. Malliakas, Zhifu Liu, John. A. Peters, Maria Sebastian, Duck Young Chung, Bruce W. Wessels, and Mercurio G. Kanatzidis*

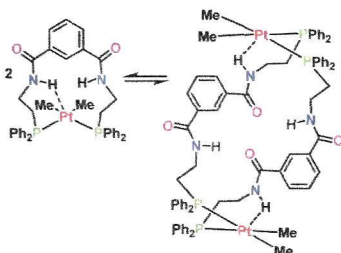
We report the crystal growth, electrical resistivity, photoconductivity properties, and Ag $K\alpha$ X-ray photoconductivity response of an antimony chalcogenide compound, SbSeI. The grown ingot samples exhibited an n-type semiconductor with resistivity of $\sim 10^5 \Omega\text{-cm}$ and a similar order of magnitude of mobility–lifetime ($\mu\tau$) products for electron and hole carriers ($\sim 10^{-4} \text{cm}^2/\text{V}$).



7051 dx.doi.org/10.1021/ic400576m

A Versatile Diphosphine Ligand: *cis* and *trans* Chelation or Bridging, with Self Association through Hydrogen Bonding
 Nasser Nasser, Aneta Borecki, Paul D. Boyle, and Richard J. Puddephatt*

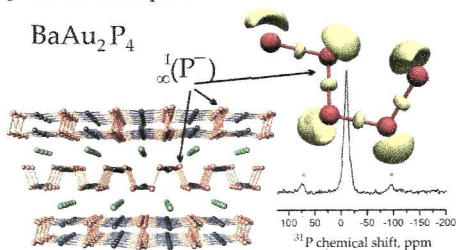
The remarkable coordination chemistry of the new diphosphine ligand, *N,N'*-bis(2-diphenylphosphinoethyl)isophthalamide, dpipa, which contains two amide groups for hydrogen bonding and which can form *cis* or *trans* chelate complexes or *cis,cis* or *trans,trans* bridged binuclear complexes, is described.



7061 dx.doi.org/10.1021/ic400584w

BaAu₂P₄: Layered Zintl Polyphosphide with Infinite $^{1-}_{\infty}(P^-)$ Chains

James Fulmer, Derrick C. Kaseman, Juli-Anna Dolyniuk, Kathleen Lee, Sabyasachi Sen, and Kirill Kovnir*
 The layered polyphosphide BaAu₂P₄ crystallizes in a new structure type with layers of Ba atoms separated by Au–P layers. The latter are composed of infinite $^{1-}_{\infty}(P^-)$ chains with a unique topology linked together by almost linearly coordinated gold atoms. According to Zintl–Klemm formalism the studied compound is electron balanced: Ba²⁺(Au⁻)₂(P⁻)₄. Magnetic and solid state NMR measurements together with quantum-chemical calculations revealed diamagnetic and semiconducting behavior of the investigated polyphosphide as expected for a Zintl phase.

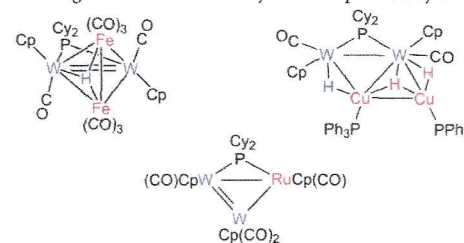


7068 dx.doi.org/10.1021/ic400602y

Heterometallic Derivatives of the Unsaturated Ditungsten Hydride [W₂(η^5 -C₅H₅)₂(H)(μ -PCy₂)(CO)₂]

M. Angeles Alvarez, M. Esther Garcia, Miguel A. Ruiz,* Adrián Toyos, and M. Fernanda Vega

Metal-hydride exchange, addition, and insertion of metal fragments are three reaction pathways to build trinuclear and tetranuclear heterometallic clusters using the title unsaturated hydride complex as a synthetic precursor.

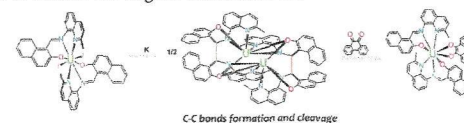


7078 dx.doi.org/10.1021/ic4006218

Synthesis of Electron-Rich Uranium(IV) Complexes Supported by Tridentate Schiff Base Ligands and Their Multi-Electron Redox Chemistry

Clément Camp, Julie Andrez, Jacques Pécaut, and Marinella Mazzanti*

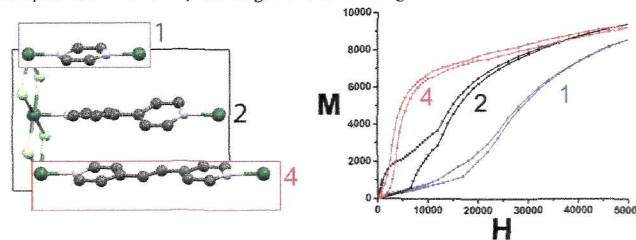
The reduction of the bis-ligand U(IV) complex of a tridentate Schiff base promotes the intramolecular C–C bond formation to afford a U(IV) amidophenolate complex which can act as a multi-electron reducing agent releasing two electrons through the cleavage of the C–C bond to restore the original imino function.



7087 dx.doi.org/10.1021/ic400632c

Modulation of the Magnetic Properties of Two-Dimensional Compounds [NiX₂(N–N)] by Tailoring Their Crystal Structure
 Miguel Cortijo, Santiago Herrero,* Reyes Jiménez-Aparicio,* and Emilio Matesanz

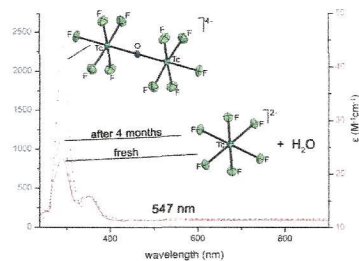
The balance between the ferromagnetic interactions along the [NiX₂] chains and the antiferromagnetic interactions between chains from different layers can be tuned by the length of the N–N ligand.



Hexafluoridotechnetate(IV) Revisited

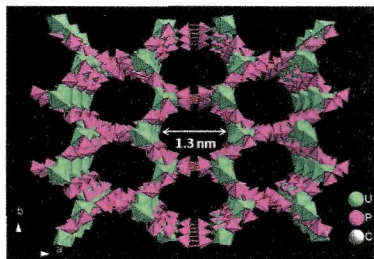
Samundeeswari Mariappan Balasekaran, Matthias Molski, Johann Spandl, Adelheid Hagenbach, Roger Alberto, and Ulrich Abram*

Novel synthetic routes for several $M_2[TcF_6]$ salts ($M = Na, K, Rb, Cs, NH_4,$ and NMe_4) were developed, and their single-crystal X-ray structures were determined. $[TcF_6]^{2-}$ salts are widely stable in aqueous solution. In alkaline media, however, a slow hydrolysis is observed, and the first hydrolysis product, the dimeric, oxido-bridged complex $[F_5Tc-O-TcF_5]^{4-}$, was isolated and studied structurally.

**Syntheses and Structures of Uranyl Ethylenediphosphonates: From Layers to Elliptical Nanochannels**

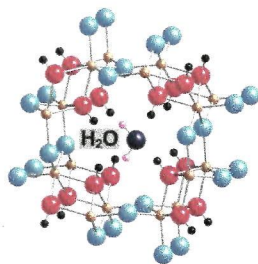
Tao Tian, Weitong Yang, Hao Wang, Song Dang, Qing-Jiang Pan, and Zhong-Ming Sun*

A series of uranium diphosphonates have been hydrothermally synthesized through the reaction of ethylenediphosphonic acid and uranyl nitrate/zinc uranyl acetate in the presence of various organic templates. EDP-U1, EDP-U2, and EDP-U3 present as layered structures. EDP-U4 is featured by large elliptical channels with the opening of $1.3 \times 1.1 \text{ nm}^2$, which represents the largest channel among the 3-D uranyl phosphonates.

**Water Vapor Diffusion into a Nanostructured Iron Oxyhydroxide**

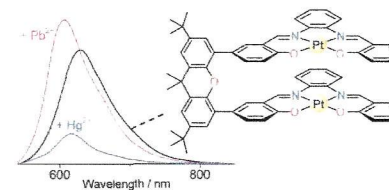
Xiaowei Song* and Jean-François Boily

This work presents the experimental and theoretical evidence for water molecule diffusion reactions into the tunnel structure of akaganéite ($\beta\text{-FeOOH}\cdot(\text{HCl})_{0.11-0.19}$). These water molecules induce important changes in the hydrogen-bonding environment of the bulk hydroxyls and can be present in the loading of up to 22.4 mg/g akaganéite.

**Crowded Bis-(M-salphen) [M = Pt(II), Zn(II)] Coordination Architectures: Luminescent Properties and Ion-Selective Responses**

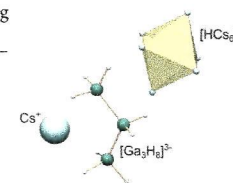
Wah-Leung Tong, Shek-Man Yiu, and Michael C. W. Chan*

A new class of rigidly linked binuclear assemblies featuring cofacial luminophore units has been developed. Their ion-selective luminescent responses have been examined, and a plausible binding mechanism involving guest-induced axial rotation of Pt-salphen moieties is proposed.

**Cs₁₀H[Ga₃H₈]₃: A Hydrogenous Zintl phase Containing Propane-Like Polyanions [Ga₃H₈]³⁻ and Interstitial Hydrogen**

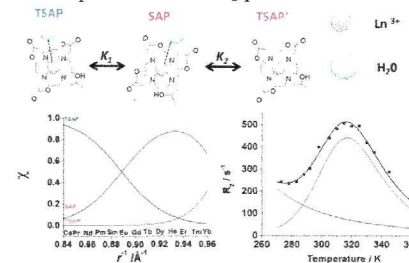
Henrik Fahlquist* and Dag Noréus

The hydrogenous Zintl-phase compound $Cs_{10}H[Ga_3H_8]_3$ synthesized by solid state processing and characterized by X-ray Powder Diffraction, Neutron Powder Diffraction, and FTIR spectroscopy. The crystal structure features three ionic species, one being the novel $[Ga_3H_8]^{3-}$ propane-like anion supported by the cations Cs^+ and $[HCs_6]^{5+}$.

**Combined High Resolution NMR and ¹H and ¹⁷O Relaxometric Study Sheds Light on the Solution Structure and Dynamics of the Lanthanide(III) Complexes of HPDO3A**

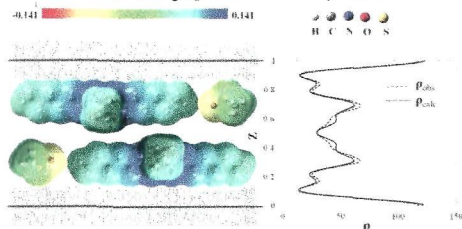
Daniela Delli Castelli, Maria C. Caligara, Mauro Botta,* Enzo Terreno, and Silvio Aime*

The chemical nature of the enantiomeric pairs present in the aqueous solutions of the lanthanide(III) complexes of HPDO3A has been elucidated. A model describing the molar fractions of the isomers as a function of the ionic radius was developed. This information has been used to reanalyze the relaxometric data of GdHPDO3A which enabled a thorough analysis of its proton relaxivity and of the anomalous shape of the VT-¹⁷O R₂ profile.



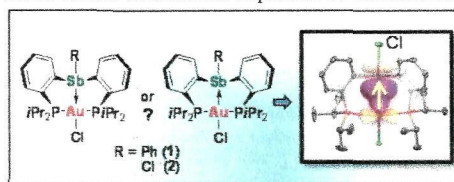
7139  dx.doi.org/10.1021/ic400733k
Preparation of a Homologous Series of Tetraalkylammonium Graphite Intercalation Compounds
 Weekit Sirisaksoontorn and Michael M. Lerner*


Graphite intercalation compounds (GICs) of a series of symmetric or asymmetric tetraalkylammonium (TAA) intercalates are obtained via cation exchange. $[(C_4H_9)_4N]C_{43}$ has flattened TAA monolayers; the larger symmetric TAA cations, $(C_6H_{13})_4N$, $(C_7H_{15})_4N$, $(C_8H_{17})_4N$, and the asymmetric TAA cations, $(C_{12}H_{25})(CH_3)_3N$, $(C_{18}H_{37})(CH_3)_3N$, $(C_{18}H_{37})_2(CH_3)_2N$, all have flattened TAA bilayers. Raman data confirm the low graphene sheet charge densities in the obtained GICs.



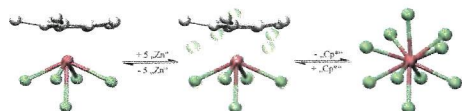
7145  dx.doi.org/10.1021/ic400736b
 σ -Donor/Acceptor-Confused Ligands: The Case of a Chlorostibine
 lou-Sheng Ke and François P. Gabbaï*

The antimony atom of the tridentate diphosphinostibine (σ -(Ph₂P)₂C₆H₄)₂SbCl behaves as a Z rather than an L ligand toward gold(I). The σ -acceptor behavior of antimony is supported by its seesaw coordination geometry as well as theoretical studies which point to the presence of a Au→Sb interaction. Through comparative studies, it is also shown that the presence of an electron withdrawing antimony-bound chloride substituent is responsible for the observed σ -accepting behavior.



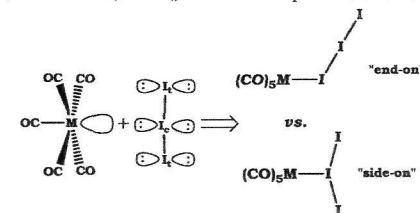
7152  dx.doi.org/10.1021/ic400741b
The Organozinc Rich Compounds $[Cp^*M(ZnR)_5]$ (M = Fe, Ru; R = Cp*, Me, Cl, Br)
 Mariusz Molon, Christian Gemel, Rüdiger W. Seidel, Paul Jerabek, Gernot Frenking,* and Roland A. Fischer*


Novel half-sandwich-type zinc-rich ruthenium complexes of general formula $[Cp^*M(ZnR)_5]$ are presented. Structural and computational investigations reveal a close relationship to the parent fully organozinc ligated compound $[Ru-(ZnCp^*)_4(ZnMe)_6]$.



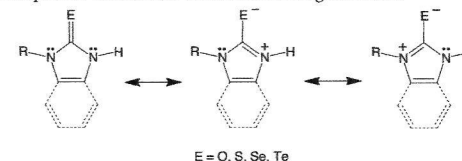
7161  dx.doi.org/10.1021/ic400772u
Hypervalent Compounds as Ligands: I₃⁻ Anion Adducts with Transition Metal Pentacarbonyls
 Andrey Yu. Rogachev and Roald Hoffmann*


Just a couple of transition metal complexes of the familiar triiodide anion are known. In this Article we report the first detailed theoretical investigation of different possible isomers of adducts of I₃⁻ with Lewis acids, $[Cr(CO)_5]$ and $[Mn(CO)_5]^+$. Both side-on and end-on complexes are calculated as bound, by 28 to 118 kcal/mol, and with ~10 kcal/mol barrier to isomerization. Orbital interactions, electrostatics, and L_nM–triiodide repulsions all enter an analysis of the bonding.



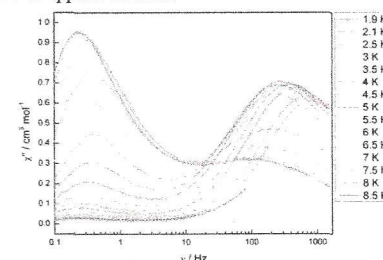
7172  dx.doi.org/10.1021/ic400786g
Structural Characterization of 2-Imidazolones: Comparison with their Heavier Chalcogen Counterparts
 Yi Rong, Ahmed Al-Harbi, Benjamin Kriegel, and Gerard Parkin*

Comparison of the C–E bond lengths of the imidazolechalcogenones with those of C–E single bonds indicates that the C–O bonds are anomalously short. A natural bond orbital (NBO) analysis of the bonding demonstrates that a doubly bonded C=E resonance structure is most significant for the oxygen derivative, whereas zwitterionic singly bonded resonance structures are dominant for the tellurium derivative. σ -Polarization for the heavier chalcogens, however, opposes the π -polarization and thereby reduces the negative charge on the chalcogen that is implied by the zwitterionic structure. As such, the C–O bond is the most polar and the ionic component contributes toward shortening the bond.



7183  dx.doi.org/10.1021/ic400789k
Single-Molecule Magnetism in Three Related $\{Co^{III}_2Dy^{III}_2\}$ -Acetylacetonate Complexes with Multiple Relaxation Mechanisms
 Stuart K. Langley, Nicholas F. Chilton, Boujemaa Moubaraki, and Keith S. Murray*

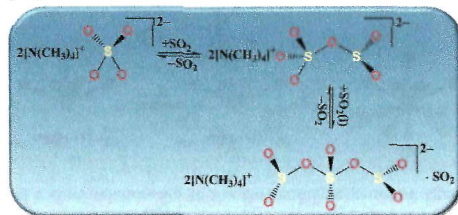
The structural and magnetic properties of tetranuclear “butterfly” complexes of the type $[Dy^{III}_2Co^{III}_2(\mu_3-OR)_2(L)_2(acac)_4(NO_3)_2]$, where L²⁻ is the dianion of triethanolamine or N-methyldiethanolamine, R = H or Me, and acac is acetylacetonate, are described in detail. Magnetically, the complexes behave as dinuclear Dy^{III} materials that display single-molecule magnetism. This Article focuses on the ac susceptibility data that revealed fast quantum tunneling below 5 K along with multiple relaxation mechanisms, the latter being sensitive to applied dc fields.



Synthesis of $[\text{N}(\text{CH}_3)_4]_2\text{O}_3\text{SOSO}_2(\text{s})$ and $[\text{N}(\text{CH}_3)_4]_2[(\text{O}_2\text{SO})_2\text{SO}_2] \cdot \text{SO}_2(\text{s})$ Containing $(\text{SO}_4)(\text{SO}_2)_x^{2-}$ $x = 1, 2$, Members of a New Class of Sulfur Oxydianions

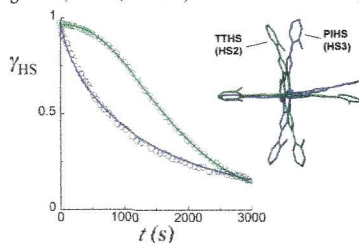
Pablo Bruna, Andreas Decken, Friedrich Grein, Jack Passmore,* J. Mikko Rautiainen, Stephanie Richardson, and Tom Whidden

One mole equivalent of SO_2 reversibly reacts with $[\text{N}(\text{CH}_3)_4]_2\text{SO}_4(\text{s})$ to give $[\text{N}(\text{CH}_3)_4]_2\text{S}_2\text{O}_6(\text{s})$ (**1**) containing $[\text{O}_3\text{SSO}_2]^{2-}$, shown by Raman and IR to be an isomer of the $[\text{O}_2\text{SSO}_3]^{2-}$ dianion. Crystals of $[\text{N}(\text{CH}_3)_4]_2(\text{O}_2\text{SO})_2\text{SO}_2 \cdot \text{SO}_2$ (**2**) were isolated from solutions of $[\text{N}(\text{CH}_3)_4]_2\text{SO}_4$ in liquid SO_2 . The X-ray structure showed that **2** contained the $[(\text{O}_2\text{SO})_2\text{SO}_2]^{2-}$ dianion. **1** and **2** are the first two members of the $(\text{SO}_4)(\text{SO}_2)_x^{2-}$ series analogous to the well-known small cation salts of the $\text{SO}_4(\text{SO}_3)_x^{2-}$ polysulfates.

**Multimetastability in a Spin-Crossover Compound Leading to Different High-Spin-to-Low-Spin Relaxation Dynamics**

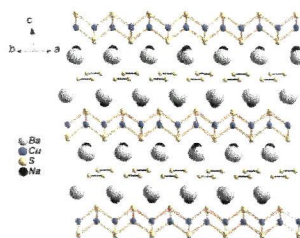
Gavin A. Craig, Jose Sánchez Costa,* Simon J. Teat, Olivier Roubeau,* Dmitry S. Yufit, Judith A. K. Howard, and Guillem Aromí*

Two different high-spin metastable states of an iron(II) complex, obtained by flash cooling and light irradiation, respectively, exhibit disparate relaxation dynamics to the low-spin ground state. The differing behavior is interpreted, in light of the structural information, in terms of the effective decoupling of a magnetic and a crystallographic phase transition through the light-induced excited-spin-state trapping effect, which, in turn, cannot be achieved by thermal trapping.

 **$\text{NaBa}_2\text{Cu}_3\text{S}_5$: A Doped p-Type Degenerate Semiconductor**

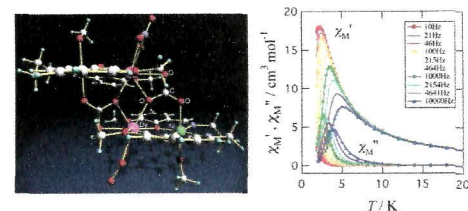
Mihai Sturza, Fei Han, Daniel P. Shoemaker, Christos D. Malliakas, Duck Young Chung, Hosub Jin, Arthur J. Freeman, and Mercouri G. Kanatzidis*

$\text{NaBa}_2\text{Cu}_3\text{S}_5$ is a p-type degenerate semiconductor with high carrier concentration, with mixed $\text{S}^{2-}/\text{S}^{1-}$ oxidation states. $\text{NaBa}_2\text{Cu}_3\text{S}_5$ features anti-PbO-type $[\text{Cu}_2\text{S}_2]$ layers intercalated with Ba, Na cations and disulfide $[\text{S}_2^{2-}]$ anions. The conductivity of single crystals is $\sim 450 \text{ S cm}^{-1}$ at room temperature while the optical band gap is 0.45 eV.

**Carbonato-Bridged $\text{Ni}^{\text{II}}_2\text{Ln}^{\text{III}}_2$ ($\text{Ln}^{\text{III}} = \text{Gd}^{\text{III}}, \text{Tb}^{\text{III}}, \text{Dy}^{\text{III}}$) Complexes Generated by Atmospheric CO_2 Fixation and Their Single-Molecule-Magnet Behavior: $[(\mu_4\text{-CO}_3)_2\{\text{Ni}^{\text{II}}(3\text{-MeOsaln})(\text{MeOH or H}_2\text{O})\text{Ln}^{\text{III}}(\text{NO}_3)_2\}]\text{-solvent}$ [3-MeOsaln = *N,N'*-Bis(3-methoxy-2-oxybenzylidene)-1,3-propanediaminato]**

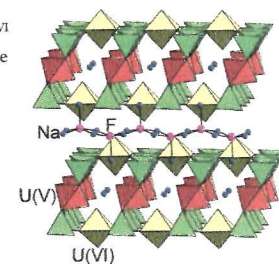
Soichiro Sakamoto, Takeshi Fujinami, Koshiro Nishi, Naohide Matsumoto,* Naotaka Mochida, Takayuki Ishida, Yukinari Sunatsuki, and Nazzareno Re

Atmospheric CO_2 fixation occurred in a mixed solution of $[\text{Ni}^{\text{II}}(3\text{-MeOsaln})(\text{H}_2\text{O})_2] \cdot 2.5\text{H}_2\text{O}$ [3-MeOsaln = *N,N'*-bis(3-methoxy-2-oxybenzylidene)-1,3-propanediaminato], $\text{Ln}^{\text{III}}(\text{NO}_3)_3 \cdot 6\text{H}_2\text{O}$, and triethylamine. The structure can be described as two di- μ -phenoxo-bridged $\text{Ni}^{\text{II}}\text{Ln}^{\text{III}}$ binuclear units bridged by two carbonato ions to form a carbonato-bridged $(\mu_4\text{-CO}_3)_2\{\text{Ni}^{\text{II}}_2\text{Ln}^{\text{III}}_2\}$ structure. The magnetic susceptibility data indicated a ferromagnetic interaction between high-spin Ni^{II} and Ln^{III} ions ($\text{Ln}^{\text{III}} = \text{Gd}^{\text{III}}, \text{Tb}^{\text{III}}, \text{Dy}^{\text{III}}$). Alternating-current susceptibility measurements indicated an out-of-phase signal for the $\text{Ni}^{\text{II}}_2\text{Tb}^{\text{III}}_2$ and $\text{Ni}^{\text{II}}_2\text{Dy}^{\text{III}}$ complexes.

**High-Temperature, High-Pressure Hydrothermal Synthesis and Characterization of a Salt-Inclusion Mixed-Valence Uranium(V,VI) Silicate: $[\text{Na}_9\text{F}_2][(\text{U}^{\text{V}}\text{O}_2)(\text{U}^{\text{VI}}\text{O}_2)_2(\text{Si}_2\text{O}_7)_2]$**

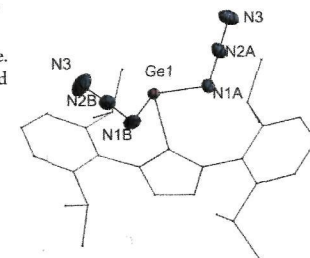
Yu-Chih Chang, Wen-Jung Chang, Sophie Boudin, and Kwang-Hwa Lii*

A salt-inclusion mixed-valence uranium(V,VI) silicate was synthesized under hydrothermal conditions at 585 °C and 160 MPa and its structure contains 2D sheets of U^{VI} disilicate which are connected by $\text{U}^{\text{V}}\text{O}_6$ tetragonal bipyramids to form thick layers. The interlayer region contains infinite chains of edge-sharing FN_3 square pyramids.

**Synthesis and Structure of Base-Stabilized Germanium(II) Diaza IPRGe(N_3)₂**

Benjamin Lyhs, Dieter Bläser, Christoph Wölper, Stephan Schulz,* Rebekka Haack, and Georg Jansen

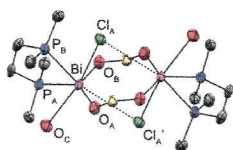
Coordination of a strong σ -Base is an effective method for the stabilization of low valent main group element complexes. Herein we report on the synthesis of IPRGe(N_3)₂ **1**, the first structurally characterized covalently bound group 14 diaza. Detailed computational studies reveal the bonding situation in homoleptic Ge(II) and Ge(IV) azides.



7242 **S** dx.doi.org/10.1021/ic400875a

Coordination Complexes of Bismuth Triflates with Tetrahydrofuran and Diphosphine Ligands
Saurabh S. Chitnis, Neil Burford,* Andreas Decken, and Michael J. Ferguson

Halobismuth triflate compounds with tetrahydrofuran or diphosphine donors have been prepared and structurally characterized as dimers in the solid state. The complexes show strong Bi–O_{OTf} interactions, classifying them as [L₂BiX₂OTf] or [L₂BiXOTf₂] complexes rather than ionic triflate salts. The reaction of [PdCl₄]²⁻ with [dmpeBiClOTf₂] gives [(dmpe)₂Pd]·[(CH₃CN)₂Bi₂Cl₆(OTf)₂], which has been structurally characterized.

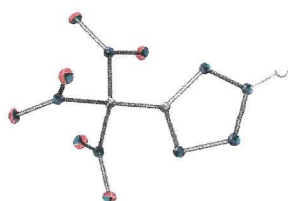


7249 **S** dx.doi.org/10.1021/ic400919n

Energetic High-Nitrogen Compounds: 5-(Trinitromethyl)-2H-tetrazole and -tetrazolates, Preparation, Characterization, and Conversion into 5-(Dinitromethyl)tetrazoles

Ralf Haiges* and Karl O. Christe

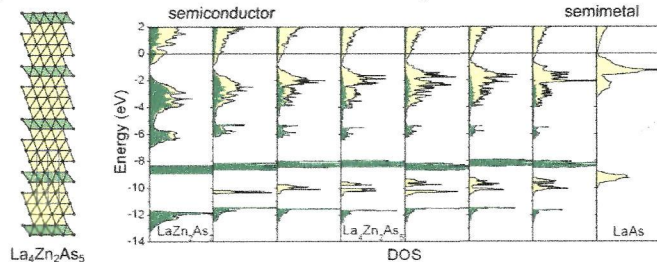
A convenient access to 5-(trinitromethyl)-2H-tetrazole (HTNTz) has been developed by the exhaustive nitration of 1H-tetrazole-5-acetic acid. HTNTz was converted into the ammonium, guanidinium, rubidium, cesium, copper and silver 5-(trinitromethyl)-2H-tetrazolates. In addition, the ammonia adducts of the copper and silver salts were isolated. The reaction of HTNTz with hydrazine and hydroxylamine resulted in the formation of hydrazinium 5-(dinitromethyl)tetrazolate and hydroxylammonium 5-(dinitromethyl)-1H-tetrazolate, respectively. Acid treatment of both 5-(dinitromethyl)tetrazolates resulted in the isolation of 5-(dinitromethylene)-4,5-dihydro-1H-tetrazole, which was converted into potassium 5-(dinitromethyl)-1H-tetrazolate by reaction with K₂CO₃. The 5-(trinitromethyl) and 5-(dinitromethyl)-tetrazoles are highly energetic materials that explode upon impact or heating.



7261 **S** dx.doi.org/10.1021/ic400933v

Homologous Series of Rare-Earth Zinc Arsenides REZn_{2-x}As₂n(REAs) (RE = La–Nd, Sm; n = 3, 4, 5, 6)
Xinsong Lin and Arthur Mar*

The intergrowth of rocksalt-type [REAs] blocks of increasing thickness within a homologous series of ternary rare-earth zinc arsenides gradually modifies the electronic structure from semiconducting to semimetallic behavior.

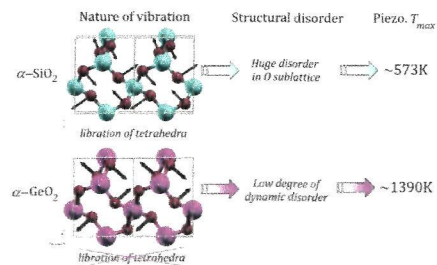


7271 dx.doi.org/10.1021/ic4009416

Vibrational Origin of the Thermal Stability in the Highly Distorted α -Quartz-Type Material GeO₂: An Experimental and Theoretical Study

Guillaume Frayssé,* Adrien Lignie, Patrick Hermet, Pascale Armand,* David Bourgoigne, Julien Haines, Bertrand Ménaert, and Philippe Papet

Polarized and variable-temperature Raman spectroscopic measurements on high-quality, water-free, flux-grown α -quartz GeO₂ single crystals combined with state-of-the-art first-principles calculations allow the controversies on the mode symmetry assignment to be solved, the nature of the vibrations to be described in detail, and the origin of the high thermal stability of this material to be explained.

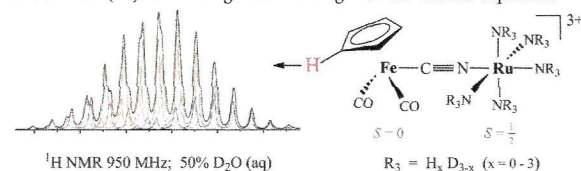


7280 **S** dx.doi.org/10.1021/ic400903a

140 H/D Isotopomers Identified by Long-Range NMR Hyperfine Shifts in Ruthenium(III) Ammine Complexes. Hyperconjugation in Ru–NH₃ Bonding

W. Michael Laidlaw,* Robert G. Denning, Jennifer C. Green, Jonathan Boyd, Jeffrey Harmer, and Amber L. Thompson

¹H NMR spectra of [(η^5 -C₅H₅)Fe(CO)₂(μ -CN)Ru(NH₃)₅](CF₃SO₃)₃, when traces of partially deuterated water are present instead of a single cyclopentadienyl resonance shifted by the hyperfine interaction, show numerous well-resolved resonances. The spectra were simulated satisfactorily by giving the appropriate statistical weight to 140 possible H/D isotopomers formed by deuteration in the five ruthenium(III) ammine ligands. The origin of the shifts is explained.

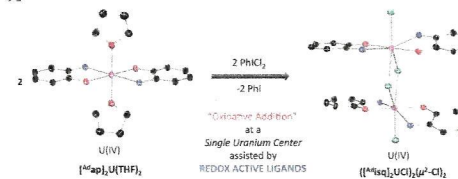


7295 **S** dx.doi.org/10.1021/ic4009812

“Oxidative Addition” of Halogens to Uranium(IV) Bis(amidophenolate) Complexes

Ellen M. Matson, Stacey R. Opperwall, Phillip E. Fanwick, and Suzanne C. Bart*

A family of U(IV) bis(amidophenolate) complexes (^Rap)₂U(THF)₂ [R = tBu (1), Ad (2), dipp (3)] have been synthesized by salt metathesis of 2 equiv of the corresponding alkali metal salt of the reduced ligand, M₂[^Rap] [M = K (tBu, Ad), Na (dipp)] with UCl₄. Addition of PhICl₂ results in ligand-assisted “oxidative” addition of the complexes to form [(^Risq)₂UCl]₂(μ^2 -Cl)₂ [R = tBu (4), Ad (5), dipp (6)].



Additions and Corrections

7305



[dx.doi.org/10.1021/ic401084w](https://doi.org/10.1021/ic401084w)

Correction to Theoretical and Experimental Investigations on Hypoelectronic Heterodimetallaboranes of Group 6

Transition Metals

Bellie Sundaram Krishnamoorthy, Arunabha Thakur, Kiran Kumar Varma Chakrahari, Shubhankar Kumar Bose, Paul Hamon, Thierry Roisnel, Samia Kahlal, Sundargopal Ghosh,* and Jean-François Halet*

7306



[dx.doi.org/10.1021/ic401300u](https://doi.org/10.1021/ic401300u)

Correction to Coordination Chemistry of 6-Thioguanine Derivatives with Cobalt: Toward Formation of Electrical Conductive One-Dimensional Coordination Polymers

Pilar Amo-Ochoa, Simone S. Alexandre, Samira Hribesh, Miguel A. Galindo, Oscar Castillo, Carlos J. Gómez-García, Andrew R. Pike, José M. Soler, Andrew Houlton,* Ross W. Harrington, William Clegg, and Félix Zamora*